EFFECT OF ORIENTATIONAL ORDER ON THE DECAY OF THE FLUORESCENCE ANISOTROPY IN MEMBRANE SUSPENSIONS

A New Approximate Solution of the Rotational Diffusion Equation

WIEB VAN DER MEER
Physiological Laboratory, University of Leiden, NL-2300 RC Leiden, The Netherlands

HANS POTTEL AND WILLY HERREMAN
Interdisciplinair Research Centrum, Katholieke Universiteit Leuven, Campus Kortrijk, B-8500 Kortrijk, Belgium

MARCEL AMELOOT AND HUBERT HENDRICKX
Limburgs Universitair Centrum, Division of Biophysics, Universitaire Campus, B-3610 Diepenbeek, Belgium

HARALD SCHRÖDER
Universität Konstanz, Fakultät für Physik, D-7750 Konstanz, Federal Republic of Germany

ABSTRACT We discussed the time-dependence of fluorescent emission anisotropy of a cylindrical probe in membrane vesicles. We showed that, if the motion of the probe were described as diffusion in an anisotropic environment, it would be possible to determine not only the second-rank but also the fourth-rank orientational order parameter from the decay of the fluorescence anisotropy. The approximations involved were based on an interpolation of short-time and long-time behavior of the relevant correlation functions. A general expression was derived for the time dependence of the fluorescence anisotropy in closed form, which applies to any particular distribution model. It was shown to be in good agreement with previously reported results for the cone model and the Gaussian model. Finally, the applicability of the theory to time-resolved and differential phase fluorescence depolarization experiments was discussed.

INTRODUCTION

Time-resolved fluorescence depolarization of probes embedded in membrane suspensions can be expected to provide detailed information about the orientational order and dynamics of these systems. Although a membrane vesicle system is isotropic as a whole, the distribution of probes is not random on a molecular scale. The molecules do not assume all possible orientations in the membrane with equal probability. Consequently the motion of a probe is restricted and the fluorescence anisotropy, $r(t)$, does not decay to zero, but reaches a finite value $r(\infty)$ (1–4). Kinosita et al., were the first to give a theoretical analysis relating the characteristics of the fluorescence anisotropy decay to membrane properties (5). To describe the motion of a cylindrical probe in a membrane, they assume that the symmetry axis of the probe tumbles isotropically within a cone of semi-angle θ_c. This model allows a quantitative interpretation of the decay of $r(t)$ in terms of a "wobbling diffusion constant" and a "degree of orientational constraint" (5). Heyn (6) and Jähnig (7) have pointed out that this degree of orientational constraint is proportional to the square of the second-rank orientational order parameter. Thus they showed that fluorescence depolarization studies in membranes may provide model-independent information about the orientational distribution of the probe.

The time-dependence of $r(t)$ reflects the dynamics of the probe that can be described as rotational diffusion in an anisotropic environment. This has been analyzed using a model-dependent approach by Kinosita et al. (5) and Lipari and Szabo (8, 9) on the basis of the cone model and by Zannoni (10, 11) taking the Gaussian model (Maier-Saupe model).

The purpose of the present paper is to introduce a

Dr. Ameloot's present address is the Department of Biology, Johns Hopkins University, Baltimore, Maryland 21213.
Address all correspondence to Dr. W. Herreman.
W. van der Meer's current address is Division of Cell Biology, Antoni van Leeuwenhoekhuis, The Netherlands Cancer Institute, 121 Plesmanlaan, 1066 CX Amsterdam, The Netherlands.

general analysis of the fluorescence anisotropy decay in membrane suspensions on the basis of the Smoluchowski equation for hindered rotational diffusion, but independent of any particular model for the distribution of the probes. We will show that the time dependence of $r(t)$ allows to determine not only the second-rank but also the fourth-rank orientational order parameter for probes with cylindrical symmetry. We introduce approximate expressions for the fluorescence anisotropy decay of a cylindrical probe in the case that both the wobbling of the symmetry axis and the rotational diffusive motion about this axis contribute to the decay.

The outline of this paper is as follows. First, a simple approximation is introduced for the fluorescence anisotropy decay of a cylindrical probe in a membrane. It is based on an interpolation of the short-time and long-time behavior of $r(t)$. The decay in this approximation contains three exponentials, but can be expressed as one or two exponentials plus a constant in special cases. Second, an improvement is proposed that consists of applying a similar interpolation procedure to the correlation functions into which $r(t)$ can be decomposed. The resulting expression for the fluorescence anisotropy depends on the diffusion constants and the second- and fourth-rank orientational order parameters. Third, the nature and limitations of our approximations are discussed and our results are compared with previous theories. Finally, we discuss the relevance of our results for interpreting fluorescence depolarization experiments with flash excitation (pulse technique) or sinusoidally modulated excitation (phase and demodulation technique).

FLUORESCENCE ANISOTROPY

First Approximation

We consider an isotropic suspension of membrane vesicles doped with fluorescent reporter molecules. The fluorescence anisotropy decay, $r(t)$, after excitation by an infinitely short flash is given by (8, 10, 12)

$$r(t) = \tfrac{2}{5}\langle\langle P_2(\mu_0 \cdot \nu_t)\rangle\rangle, \tag{1}$$

where $P_2(x) = \tfrac{3}{2}x^2 - \tfrac{1}{2}$ is the second Legendre polynomial and $\mu_0 \cdot \nu_t$ is the inner product of μ_0, a unit vector along the absorption dipole at zero time, with ν_t, a unit vector along the emission dipole at time t. It is assumed here that the absorption and emission are each characterized by a single transition moment. The double brackets in Eq. 1 denote an ensemble average over the orientations of the probes at time zero and time t (see Appendix A). The decay of the fluorescence intensities following an excitation that is not an infinitely short flash, can be obtained by deconvoluting with the response function of the fluorometer.

We assume that the label distribution is axially symmetric around the membrane normal, which is called the director. We define a local coordinate system (X_D, Y_D, Z_D), the director frame, of which the Z_D-axis points along the local membrane normal. A coordinate system (X_M, Y_M, Z_M), the molecular frame, is fixed in the fluorophore. The director frame can be rotated into the molecular frame at time t by the Euler angles (Φ_t, θ_t, Ψ_t, where Φ_t is the azimuthal angle of the Z_M-axis in the director frame, θ_t is the corresponding polar angle, i.e., the angle between Z_M and Z_D, and Ψ_t is the angle between the Y_M-axis and the line intersecting the X_D, Y_D) and (X_M, Y_M) planes. The absorption and emission dipoles are assumed to have a fixed orientation in the molecular frame; θ_μ and θ_ν are the polar angles of the absorption and emission dipole, respectively, and Φ_μ and Φ_ν are the corresponding azimuthal angles, as shown in Fig. 1.

Our analysis applies to probes having effectively cylindrical symmetry. The symmetry axis is taken along Z_M. Because the orientational distribution of the probe is assumed to be axially symmetric around Z_D, it depends only on θ and not on Φ or Ψ. The probability that the angle between the director and the molecular axis has a value between θ and $\theta + d\theta$ can be written as $f(\theta)\sin\theta d\theta$, where $f(\theta)$ is the orientational distribution of the probe. This function can be expanded in a series of Legendre polynomials

$$f(\theta) = \frac{1}{2} + \sum_{l=1}^{\infty} \frac{4l+1}{2}\langle P_{2l}\rangle P_{2l}(\cos\theta) \tag{2}$$

where the coefficients are given by

$$\langle P_{2l}\rangle = \int_0^\pi P_{2l}(\cos\theta) f(\theta)\sin\theta\, d\theta. \tag{3}$$

The distribution is symmetric with respect to the membrane plane, i.e., $f(\theta) = f(\pi - \theta)$, so that only even Legendre polynomials appear in Eq. 2. In an isotropic system, all $\langle P_{2l}\rangle$ are equal to zero. If all probe molecules point along the membrane normal, all $\langle P_{2l}\rangle$ are equal to unity. The distribution is completely specified if all the order parameters, $\langle P_{2l}\rangle$, are known. In practice, not all the

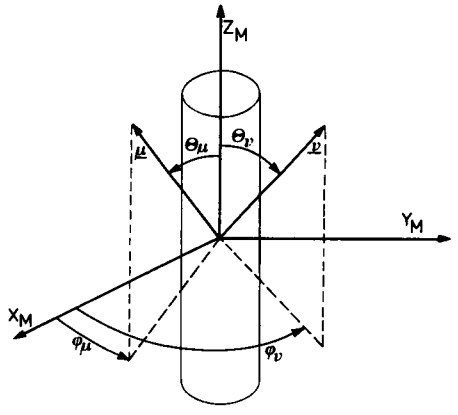

FIGURE 1 The angular coordinates of the absorption (μ) and emission (ν) dipole of the probe in the molecular frame.

order parameters can be extracted from experimental data. However, if a limited number of order parameters are known, a justified guess can be made using information theory (13). For example if only $\langle P_2 \rangle = \langle \frac{3}{2} \cos^2 \theta - \frac{1}{2} \rangle$ and $\langle P_4 \rangle = \langle \frac{35}{8} \cos^4 \theta - \frac{30}{8} \cos^2 \theta + \frac{3}{8} \rangle$ are known, the most probable distribution has the form

$$f(\theta) \sim \exp [\lambda_2 P_2(\cos \theta) + \lambda_4 P_4(\cos \theta)], \quad (4)$$

where λ_2 and λ_4 are chosen such that Eq. 3 holds for $l = 1$ and $l = 2$.

The dependence on the angular coordinates of $r(t)$, as given by Eq. 1, has been evaluated by Zannoni (10)

$$\begin{aligned} r(t) = {} & \tfrac{2}{5} P_2(\cos \theta_\mu) P_2(\cos \theta_\nu) G_0(t) \\ & + \tfrac{3}{10} \sin 2\theta_\mu \sin 2\theta_\nu \cos \Phi_{\mu\nu} G_1(t) \\ & + \tfrac{3}{10} \sin^2 \theta_\mu \sin^2 \theta_\nu \cos 2\Phi_{\mu\nu} G_2(t), \end{aligned} \quad (5)$$

where $\Phi_{\mu\nu} = \Phi_\mu - \Phi_\nu$. The correlation functions $G_n(t)$ ($n = 0, 1, 2$) are defined as

$$G_n(t) = \langle \langle D^2_{nn}(\Phi_{0t} \theta_{0t} \Psi_{0t}) \rangle \rangle, \quad (6)$$

where $D^2_{nn}(\Phi\theta\Psi)$ are elements of the Wigner rotation matrices (10, 11) (see also Appendix A) and the Euler angles $(\Phi_{0t}, \theta_{0t}, \Psi_{0t})$ take the molecular frame at time 0 into that at time t. The $G_n(t)$ have the following properties (10, 11)

$$G_n(0) = 1 \quad (7a)$$

$$G_n(\infty) = \langle P_2 \rangle^2 \delta_{n,0} \quad (7b)$$

$$\dot{G}_n(0) = -6D_\perp - (D_\parallel - D_\perp) n^2, \quad (7c)$$

where the dot denotes a time derivative and $\delta_{n,0}$ is the Kronecker delta. $D_\perp$ and $D_\parallel$ are components of the rotational diffusion tensor of the probe; $D_\perp$ is the average diffusion coefficient for the wobbling motion of the symmetry axis, and $D_\parallel$ is the average diffusion constant corresponding to rotation around this axis.

A simple interpolation formula for the fluorescence anisotropy, consistent with the properties of Eq. 7, can be constructed

$$\begin{aligned} r(t) = {} & \tfrac{2}{5} P_2(\cos \theta_\mu) P_2(\cos \theta_\nu) \{ \langle P_2 \rangle^2 \\ & + (1 - \langle P_2 \rangle^2) \exp [-6D_\perp t / (1 - \langle P_2 \rangle^2)] \} \\ & + \tfrac{3}{10} \sin 2\theta_\mu \sin 2\theta_\nu \cos \Phi_{\mu\nu} \exp (-D_\parallel t - 5D_\perp t) \\ & + \tfrac{3}{10} \sin^2 \theta_\mu \sin^2 \theta_\nu \cos 2\Phi_{\mu\nu} \exp (-4D_\parallel t - 2D_\perp t). \end{aligned} \quad (8)$$

This expression differs somewhat from the corresponding formula quoted by Lipari and Szabo (8) (their Eq. 30); their expression contains five exponentials of which three depend explicitly on $\langle P_2 \rangle$, whereas the one proposed in Eq. 8 has three exponentials of which only one exhibits a $\langle P_2 \rangle$-dependence.

Eq. 8 reduces to a more simple expression in special cases. (*a*) Reorientations around the symmetry axis dominate, if the order is (nearly) complete, $\langle P_2 \rangle \simeq 1$. Then one expects that $D_\parallel$ vanishes. Consequently, the fluorescence anisotropy of Eq. 8 becomes

$$\begin{aligned} r(t) = {} & \tfrac{2}{5} P_2(\cos \theta_\mu) P_2(\cos \theta_\nu) \langle P_2 \rangle^2 \\ & + \tfrac{3}{10} \sin 2\theta_\mu \sin 2\theta_\nu \cos \phi_{\mu\nu} \exp (-D_\parallel t) \\ & + \tfrac{3}{10} \sin^2 \theta_\mu \sin^2 \theta_\nu \cos 2\phi_{\mu\nu} \exp (-4D_\parallel t). \end{aligned} \quad (9)$$

(*b*) Reorientations of the symmetry axis dominate. This case corresponds to θ_μ and/or θ_ν being small. Then $r(t)$ of Eq. 8 reduces to

$$\begin{aligned} r(t) = r_{g1}(t) = {} & \tfrac{2}{5} P_2(\cos \theta_\mu) P_2(\cos \theta_\nu) \\ & \cdot \{ \langle P_2 \rangle^2 + (1 - \langle P_2 \rangle^2) \exp [-6D_\perp t / (1 - \langle P_2 \rangle^2)] \}. \end{aligned} \quad (10)$$

This expression is called $r_{g1}(t)$ in reference 14. Note that Eqs. 8–10 yield the exact $r(0)$ and $r(\infty)$ and the correct slope at zero time independent of the distribution model. Moreover, Eq. 8 also contains the correct expression $r(t)$ in the isotropic limit ($\langle P_2 \rangle = \langle P_4 \rangle = 0$).

Second Approximation

Experimentally it has been found that the decay of the fluorescence anisotropy is not always monoexponential (1, 2), even if the absorption dipole or the emission dipole is coaxial with the symmetry axis of the label. An improved approximation may be obtained as follows. By using the closure for the elements of the Wigner rotation matrices, the functions $G_n(t)$ can each be decomposed into three correlation functions (10, 11). These correspond to three different modes of reorientation, although difficult to visualize.

$$G_n(t) = G_{0n}(t) + 2G_{1n}(t) + 2G_{2n}(t) \quad (11)$$

where the $G_{mn}(t)$ are defined as

$$G_{mn}(t) = \langle \langle D^2_{mn}(\Phi_0 \theta_0 \Psi_0)^* D^2_{mn}(\Phi_t \theta_t \Psi_t) \rangle \rangle. \quad (12)$$

The Eular angles $(\Phi_t \theta_t \Psi_t)$ describe here the rotation that takes the director frame into the molecular frame at time t. Interpolating for each n and m ($m, n = 0, 1, 2$) the short-time behavior, $G_{mn}(t) = G_{mn}(0) + t\,\dot{G}_{mn}(0)$, with the long-time tail, $G_{mn}(t) = \langle P_2 \rangle^2 \delta_{m0} \delta_{n0}$, we obtain

$$\begin{aligned} r(t) = {} & \tfrac{2}{5} P_2(\cos \theta_\mu) P_2(\cos \theta_\nu) [\langle P_2 \rangle^2 \\ & + \beta_{00} \exp (-\alpha_{00} t) + 2 \sum_{m=1}^{2} \beta_{m0} \exp (-\alpha_{m0} t)] \\ & + \tfrac{3}{10} \sin 2\theta_\mu \sin 2\theta_\nu \cos \Phi_{\mu\nu} [\beta_{01} \exp (-\alpha_{01} t) \\ & + 2 \sum_{m=1}^{2} \beta_{m1} \exp (-\alpha_{m1} t)] \\ & + \tfrac{3}{10} \sin^2 \theta_\mu \sin^2 \theta_\nu \cos 2\Phi_{\mu\nu} [\beta_{02} \exp (-\alpha_{02} t) \\ & + 2 \sum_{m=1}^{2} \beta_{m2} \exp (-\alpha_{m2} t)], \end{aligned} \quad (13)$$

where the exponents and preexponentials are given in Table I.

The results for $\beta_{mn} = G_{mn}(0) - G_{mn}(\infty)$ have been derived by Zannoni (10). Szabo (20) has obtained the result $\dot{G}_{00}(0) = -\alpha_{00}\beta_{00}$. The derivation of $\dot{G}_{mn}(0) = -\alpha_{mn}\beta_{mn}$ is an extension thereof and can be found in Appendix A. Note that $\dot{G}_n(0) = \dot{G}_{0n}(0) + 2\dot{G}_{1n}(0) + 2\dot{G}_{2n}(0) = -6D_\perp - (D_\parallel - D_\perp)n^2$ $(n = 0, 1, 2)$ in agreement with Eq. 7c. In this approximation $D_\perp$ and $D_\parallel$ determine the decay at short times, $\langle P_2 \rangle$ at long times and $\langle P_2 \rangle$, $\langle P_4 \rangle$, $D_\perp$, and $D_\parallel$ at intermediate times. Consider again the special cases: (*a*) Reorientations around the symmetry axis dominate, if the order is (nearly) complete, $\langle P_2 \rangle \simeq \langle P_4 \rangle \simeq 1$. The $r(t)$ of Eq. 13 reduces to Eq. 9. Note that now this expression is obtained independent of any assumptions about $D_\perp$. (*b*) Reorientations of the symmetry axis dominate, if θ_μ and/or θ_ν are small. In this case the $r(t)$ of Eq. 13 becomes

$$r(t) = r_{g3}(t) = \tfrac{2}{5} P_2(\cos\theta_\mu) P_2(\cos\theta_\nu) \cdot [\langle P_2 \rangle^2 + \beta_{00} \exp(-\alpha_{00}t) + 2\sum_{m=1}^{2} \beta_{m0} \exp(-\alpha_{m0}t)]. \quad (14)$$

This expression is called $r_{g3}(t)$ in reference 14.

Also the second approximation for $r(t)$ (Eq. 13) yields the exact expressions for $r(0)$, $\dot{r}(0)$, $r(\infty)$, and $r(t)$ in the case $\langle P_2 \rangle = \langle P_4 \rangle = 0$. A few examples for the time dependence in the case $\theta_\mu = \theta_\nu = 0$ are shown in Fig. 2 *a*. Corresponding distribution functions are plotted in Fig. 2 *b*.

These distributions are not the only possible functions, but are examples that have the same $\langle P_2 \rangle$ and $\langle P_4 \rangle$ values as the corresponding decays in Fig. 2 *a*. A fluorescence anisotropy decay curve can be conveniently represented as a point in the $\langle P_2 \rangle$ $\langle P_4 \rangle$ plane, as indicated in Fig. 3.

JUSTIFICATION OF THE APPROXIMATIONS

The monoexponential formula for a correlation function, $G_{mn}(t)$, introduced above, can be considered as an approximate solution of the Smoluchowski equation as is shown in Appendix B. There it is derived from a linearization around the equilibrium value of the correlation function. The approximation is accurate if $G_{mn}(t) - G_{mn}(\infty)$ is small compared with unity and/or the time-derivative varies linearly with $G_{mn}(t) - G_{mn}(\infty)$. The maximal value of $G_{mn}(t) - G_{mn}(\infty)$ is 0.2 at $t = 0$ and decays to zero, if t approaches infinity, indicating that the mono-exponential approximation is valid, especially for larger times. In addition, it is exact near $t = 0$ and $t = \infty$ and assumes the correct behavior in the limits of complete order ($\langle P_{2n} \rangle = 1$, $n = 1, 2, 3, \ldots$) and complete disorder ($\langle P_{2n} \rangle = 0$, $n = 1, 2, 3, \ldots$). A small deviation from the exact decay may be expected at intermediate $\langle P_2 \rangle$ values. To check the validity of the approximation, the values for the area under the correlation functions are compared with the exact values in Fig. 4 for the Gaussian-model and the cone-model. The area A_{mn} $(m, n = 0, 1, 2)$ is calculated according to

$$A_{mn} = \int_0^\infty dt\, [G_{mn}(t) - \langle P_2 \rangle^2 \delta_{m0}\, \delta_{n0}]. \quad (15)$$

In the Gaussian model, or Maier-Saupe model, the reorientational potential appearing in the Smoluchowski equation is taken proportional to P_2 (cos θ) (10, 15, 16). In this model $\langle P_4 \rangle$ can be calculated, if $\langle P_2 \rangle$ is known (16). $\langle P_2 \rangle$ and $\langle P_4 \rangle$ values for the Gaussian model are given in Fig. 3. These have been used to calculate A_{m0} $(m = 0, 1, 2)$ in the second approximation for this model from Eqs. 14 and 15 and Table I, and are shown in Fig. 4 *a* together with the exact A_{m0} $(m = 0, 1, 2)$ taken from reference 17.

TABLE I
EXPONENTS AND PREEXPONENTIALS OF THE FLUORESCENCE ANISOTROPY IN THE SECOND APPROXIMATION

m	β_{mo}	α_{mo}
0	$\frac{1}{5} + 2\langle P_2 \rangle/7 + 18\langle P_4 \rangle/35 - \langle P_2 \rangle^2$	$6D_\perp(\frac{1}{5} + \langle P_2 \rangle/7 - 12\langle P_4 \rangle/35)/\beta_{00}$
1	$\frac{1}{5} + \langle P_2 \rangle/7 - 12\langle P_4 \rangle/35$	$6D_\perp(\frac{1}{5} + \langle P_2 \rangle/14 + 8\langle P_4 \rangle/35)/\beta_{10}$
2	$\frac{1}{5} - 2\langle P_2 \rangle/7 + 3\langle P_4 \rangle/35$	$6D_\perp(\frac{1}{5} - \langle P_2 \rangle/7 - 2\langle P_4 \rangle/35)/\beta_{20}$
	β_{m1}	α_{m1}
0	$\frac{1}{5} + \langle P_2 \rangle/7 - 12\langle P_4 \rangle/35$	$D_\perp(1 + 2\langle P_2 \rangle/7 + 12\langle P_4 \rangle/7)/\beta_{01} + D_\parallel$
1	$\frac{1}{5} + \langle P_2 \rangle/14 + 8\langle P_4 \rangle/35$	$D_\perp(1 + \langle P_2 \rangle/7 - 8\langle P_4 \rangle/7)/\beta_{11} + D_\parallel$
2	$\frac{1}{5} - \langle P_2 \rangle/7 - 2\langle P_4 \rangle/35$	$D_\perp(1 - 2\langle P_2 \rangle/7 + 2\langle P_4 \rangle/7)/\beta_{21} + D_\parallel$
	β_{m2}	α_{m2}
0	$\frac{1}{5} - 2\langle P_2 \rangle/7 + 3\langle P_4 \rangle/35$	$D_\perp(\frac{2}{5} + 2\langle P_2 \rangle/7 - 24\langle P_4 \rangle/35)/\beta_{02} + 4D_\parallel$
1	$\frac{1}{5} - \langle P_2 \rangle/7 - 2\langle P_4 \rangle/35$	$D_\perp(\frac{2}{5} + \langle P_2 \rangle/7 + 16\langle P_4 \rangle/35)/\beta_{12} + 4D_\parallel$
2	$\frac{1}{5} + 2\langle P_2 \rangle/7 + \langle P_4 \rangle/70$	$D_\perp(\frac{2}{5} - 2\langle P_2 \rangle/7 - 4\langle P_4 \rangle/35)/\beta_{22} + 4D_\parallel$

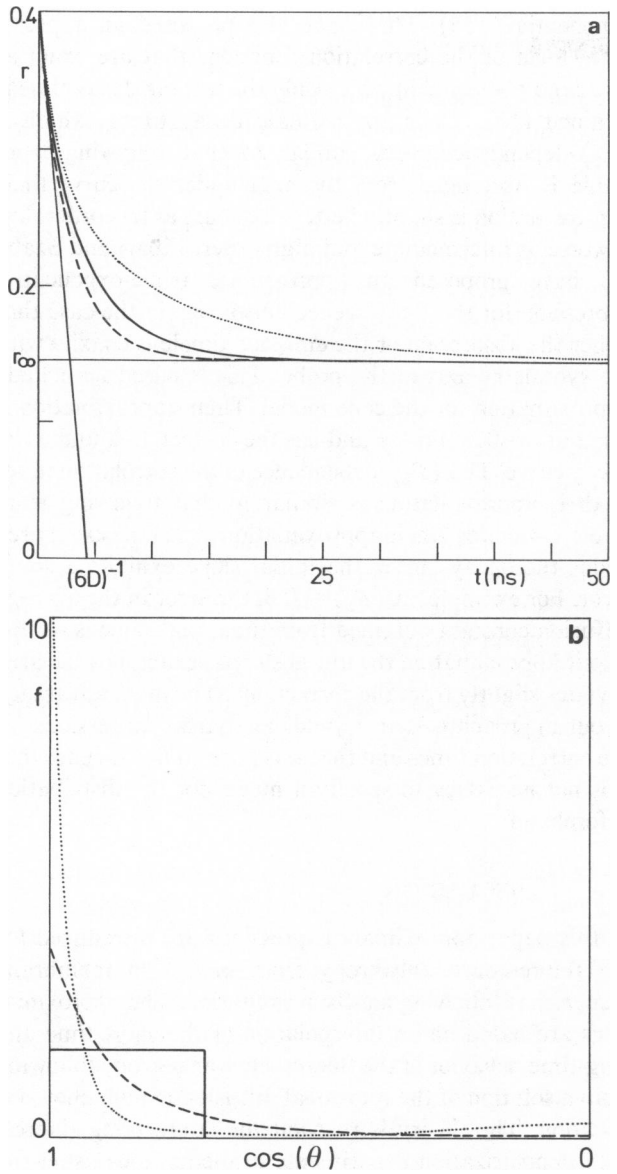

FIGURE 2 (*a*) The second approximation for $r(t)$ as a function of t in the case that $\theta_\mu = 0$ or $\theta_\nu = 0$. The slope at $t = 0$ satisfies $\dot{r}(0) = -6D_\perp r(0)$. For the same values of $r(0) = 0.400$, $\langle P_2 \rangle = 0.605$, and $D_\perp = 0.04$ ns^{-1}, three different $r(t)$ decays are shown, according to three different $\langle P_4 \rangle$ values. The dashed curve corresponds to the Gaussian model, $\langle P_4 \rangle = 0.247$, the solid curve refers to the cone model, $\langle P_4 \rangle = 0.077$, and for the dotted curve $\langle P_4 \rangle = 0.540$. (*b*) Three distribution functions $f(\theta)$ corresponding to the decay curves in Fig. 2 *a*. In all cases $\langle P_2 \rangle$ is equal to 0.605, solid curve: cone model with $\langle P_4 \rangle = 0.077$, dashed curve: Gaussian model with $\langle P_4 \rangle = 0.247$, and the dotted curve is an example of a distribution exhibiting two maxima at $\theta = 0°$ and at $\theta = 90°$ according to Eq. 4.

In the cone model, where the probe is assumed to wobble within a cone of semiangle θ_c, $\langle P_2 \rangle$ and $\langle P_4 \rangle$ are given by

$$\langle P_2 \rangle = \tfrac{1}{2} \cos \theta_c (1 + \cos \theta_c) \quad (16a)$$

$$\langle P_4 \rangle = \tfrac{1}{8} \cos \theta_c (1 + \cos \theta_c)(7 \cos^2 \theta_c - 3). \quad (16b)$$

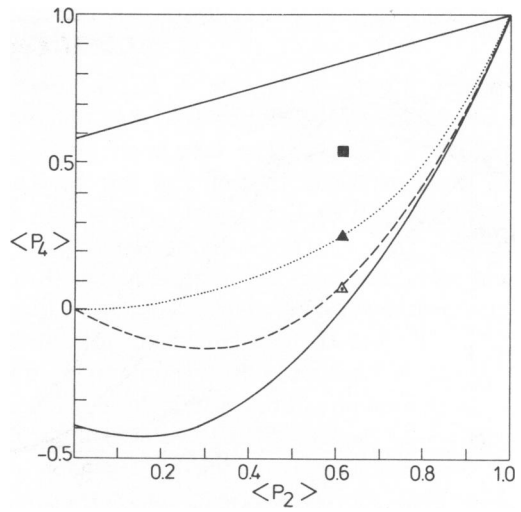

FIGURE 3 The $\langle P_2 \rangle$ $\langle P_4 \rangle$ plane with the points corresponding to the decay curves in Fig. 2 *a* with $\langle P_2 \rangle = 0.605$ and $\langle P_4 \rangle = 0.077$ (▲, cone model), $\langle P_4 \rangle = 0.247$ (▲, Gaussian model), and $\langle P_4 \rangle = 0.540$ (■), respectively. The solid lines in the plane indicate the theoretical upper ($\langle P_4 \rangle = (7 + 5 \langle P_2 \rangle)/12$) and lower limits [$\langle P_4 \rangle = (35 \langle P_2 \rangle^2 - 10 \langle P_2 \rangle - 7)/18$] (22). For comparison the relation between $\langle P_2 \rangle$ and $\langle P_4 \rangle$ are also shown for the cone model (---) and the Gaussian model (· · ·).

Using these relations A_{m0} values ($m = 0, 1, 2$) have been calculated in the second approximation. Results are shown in Fig. 4 *b* and compared with exact A_{m0} values, calculated by Lipari and Szabo (9). The agreement between the exact and approximate areas under the correlation functions is excellent for both models except for A_{10} in the cone model near $\theta_c = 90°$. The reason for this difference is that $G_{10}(t)$ deviates significantly from a mono-exponentially decaying function near $\theta_c = 90°$ (9). This is probably an artefact of the cone model, because in an isotropic system, all correlation functions should be monoexponential.

The first approximation gives a formula for the whole fluorescence anisotropy decay, independent of the $\langle P_4 \rangle$-value and can therefore not distinguish between different models. In the case that either the absorption or the emission dipole is coaxial with the symmetry axis, the fluorescence anisotropy is determined by only two parameters, $\langle P_2 \rangle$ and $D_\perp$. This is in agreement with the conclusion of Kinosita et al. (18), that the choice of a model is not crucial, when only two parameters are extracted from the anisotropy data. However, the fluorescence anisotropy in the exact calculation as well as in the second approximation, is sensitive to the choice of the model, that is, to the $\langle P_4 \rangle$ value at given $\langle P_2 \rangle$. This is clear from inspection of Table II, where the areas under the decay curves in the case $\theta_\mu = 0$ or $\theta_\nu = 0$ are given in the second approximation and from an exact calculation for the Gaussian model and for the cone model.

The second approximation appears to be accurate for both distributions. If at a certain value for $\langle P_2 \rangle$, the correct $\langle P_4 \rangle$ and $D_\perp$ would be known, Eq. 14 would predict

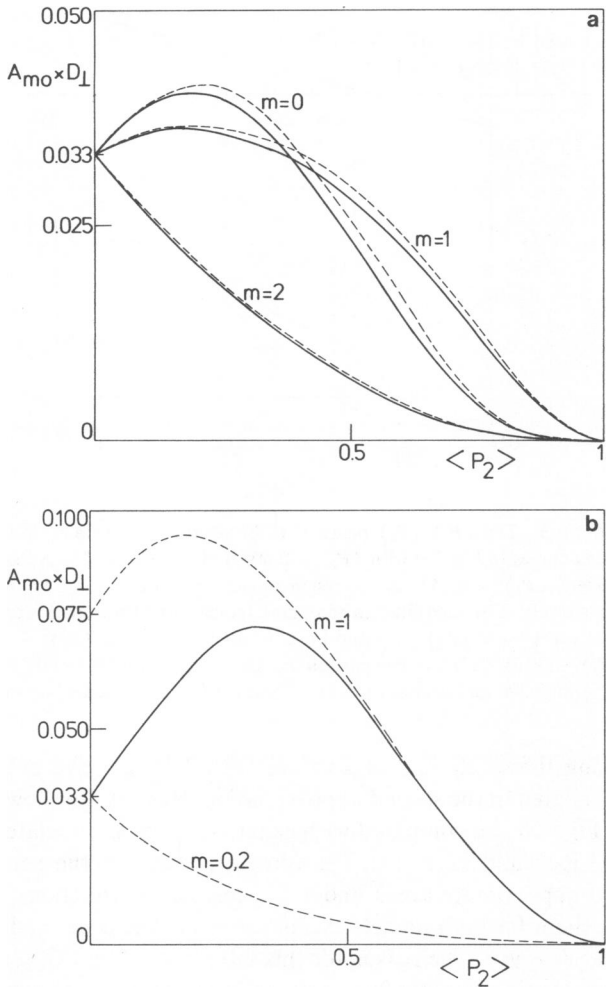

FIGURE 4 (*a*) The areas under the correlation functions, A_{m0}, m = 0, 1, 2 for the Gaussian model, exact from reference 17 (---) and approximate using Eqs. 15, A14 and Table I (——). (*b*) The areas under the correlation functions, A_{m0}, m = 0, 1, 2, for the cone model, exact from reference 9 (---) and approximate using Eqs. 15, A14 and Table I (——). For m = 0 and m = 2 the exact A_{m0} coincide with each other and with the corresponding approximate values.

a decay deviating only slightly from the exact one. Consequently, fitting experimental data to Eq. 14 would yield a $\langle P_4 \rangle$ or $D_\perp$ value that is somewhat in error. The deviations are of the order of 0.05 in $\langle P_4 \rangle$ and 10% in $D_\perp$. The experimental inaccuracy in $\langle P_4 \rangle$ found when nanosecond fluorescence anisotropy data are fitted to Eq. 14, is also of the order of 0.05 and the errors in $D_\perp$ are in general larger than 10% (14). This indicates that a determination of $\langle P_4 \rangle$, in addition to $\langle P_2 \rangle$, from time-resolved fluorescence anisotropy decay measurements in membrane suspensions is feasible and that our interpolation formula is sufficient for that purpose.

It is also of interest to compare our results with previously published approximations. Nordio and Segre have calculated the correlation functions that contribute to $r(t)$ nummerically for the Gaussian model and have shown that these can be written as a sum of an infinite number of exponentials (15). They have also proposed an approximate form of the correlation functions that are exact at $t = 0$ and $t = \infty$ and in which only the leading decay time is retained (15). Their approximate decay times exhibit a $\langle P_2 \rangle$-dependence, very similar to that following from Table I. As judged from the area under the curve their approximation is slightly better than ours at low order, but is worse at intermediate and high order. Lipari and Szabo (9) have proposed an approximate triple-exponential expression for the fluorescence anisotropy in the case that either the absorption or the emission dipole is coaxial with the symmetry axis of the probe. This is based on a Pade approximation for the cone model. Their approximation is exact at $t = 0$ and $t = \infty$ and has the correct area under the decay curve. The $\langle P_2 \rangle$-dependence of the correlation times in their approximation is similar to that following from Table I. Whereas their approximation yields the exact area under the decay curve, the initial slope exhibits a small error. For example, at $\langle P_2 \rangle = 0.4$, the error in the average diffusion constant obtained from the initial slope is ~10%. In our approximation the initial slope is exact, but the area deviates slightly from the correct one. The main advantage of our approach is that it yields analytical expressions for the correlation times and that it is general in the sense that it is not necessary to specify a model for the distribution beforehand.

DISCUSSION

In this paper approximate expressions are introduced for the fluorescence anisotropy from probes in membrane suspensions following a δ-flash excitation. The approximations are based on an interpolation of the short-time and long-time behavior of the fluorescence anisotropy following from a solution of the rotational diffusion (Smoluchowski) equation. The theory is relevant for interpreting fluorescence depolarization experiments in membranes using (*a*) flash excitation (pulse technique) and (*b*) sinusoidally modulated excitation (phase and demodulation technique). These two cases will be briefly discussed below.

(*a*) By comparing time-resolved fluorescence anisotropy data from the pulse technique with Eq. 8 (first approximation), it is possible to extract the diffusion constants $D_\perp$ and $D_\parallel$ and the second-rank orientational order parameter $\langle P_2 \rangle$ from the experimental results. $D_\parallel$ cannot be obtained for probes of which either the absorption or the emission dipole is collinear with the symmetry axis. The rodlike probes 1,6-diphenyl-1,3,5-hexatriene (DPH) and 1-[4-(trimethylamino)-6-phenyl]-6-phenyl-1,3,5-hexatriene (TMA-DPH) belong to this category. For such probes the first approximation yields an expression for the fluorescence anisotropy consisting of one exponential plus a constant (Eq. 10). It has been shown, however, that this simple model is inadequate for DPH (1, 2, 14) and an improved model is necessary such as the one of Eq. 14 (second approximation). Indeed, this expression has been

TABLE II
ORDER PARAMETERS AND THE AREAS UNDER THE DECAY CURVE FOR THE GAUSSIAN MODEL AND THE CONE MODEL

Gaussian model				Cone model		
$\langle P_2 \rangle$	$\langle P_4 \rangle$	$D_\perp \times$ Area, exact	$D_\perp \times$ Area, approximate	$\langle P_4 \rangle$	$D_\perp \times$ Area, exact	$D_\perp \times$ Area, approximate
0.334*	0.073	0.138*	0.133	−0.128	0.199‡	0.172
0.375§	0.091	0.131§	0.125	−0.117	0.184‡	0.165
0.452§	0.133	0.114§	0.107	−0.078	0.154‡	0.146
0.528§	0.184	0.095§	0.088	−0.014	0.123‡	0.120
0.605*	0.247	0.074*	0.068	0.077	0.092‡	0.091
0.677§	0.320	0.055§	0.050	0.188	0.066‡	0.064
0.819*	0.526	0.020*	0.019	0.481	0.023‡	0.021

Area = $A_\infty + 2A_{10} + 2A_{20}$, exact area values have been obtained from references 8, 15, and 18, approximate values have been calculated from Eqs. 15, A14, and Table I.

*Exact area values obtained from reference 15.

‡Exact area values obtained from reference 8.

§Exact area values obtained from reference 18.

shown to describe experimental data for DPH and TMA-DPH quite well (14). By fitting time-resolved fluorescence anisotropy data to Eq. 14, it is thus possible to measure not only the wobbling diffusion constant, $D_\perp$, and the second-rank order parameter, $\langle P_2 \rangle$, but also the fourth-rank order parameter, $\langle P_4 \rangle$ (14). These order parameters describe the distribution of the probes: $\langle P_2 \rangle$ gives the primary and $\langle P_4 \rangle$ the secondary information on orientational order. Knowledge of both parameters enables one to discriminate between distributions that would be indistinguishable if only $\langle P_2 \rangle$ would be known (11).

(*b*) Differential polarized phase fluorometry can be employed to study limited rotational motion in membranes (4, 19). Lakowicz et al. have shown that differential phase measurements at one single frequency in combination with steady state anisotropy measurements can be used to obtain values for the limiting fluorescence anisotropy and the rate of rotation of DPH, if a model like the one of Eq. 10 was taken for the time dependence of the fluorescence anisotropy (4). An extension of this approach would be to obtain the order parameters $\langle P_2 \rangle$ and $\langle P_4 \rangle$ and the wobbling diffusion constant $D_\perp$ from differential phase measurements at more than a few frequencies using the second approximation (Eq. 14). The relevant formulas are given in Appendix C for the most common case that either the absorption or the emission dipole points along the symmetry axis of the probe.

APPENDIX A

Here we derive expressions for the short-time behavior of $G_{mn}(t)$ $(m, n = -2, -1, 0, 1, 2)$

$$G_{mn}(t) = \langle\langle D^2_{mn}(\Omega_0)^* D^2_{mn}(\Omega)\rangle\rangle = \frac{1}{4\pi^2}\int d\Omega_0 \int d\Omega D^2_{mn}(\Omega_0)^* P(\Omega_0 0 \,|\, \Omega t) D^2_{mn}(\Omega) f(\theta_0), \quad \text{(A1)}$$

where the double brackets are defined and $\Omega_t = \Omega$ denotes the Eular angles $(\Phi_t \theta_t \Psi_t) = (\Phi\theta\Psi)$ that take the director frame into the molecular frame at time t. It is understood that

$$\int d\Omega = \int_0^{2\pi} d\Psi \int_0^{2\pi} d\Phi \int_0^{\pi} d\theta \sin\theta. \quad \text{(A2)}$$

The Wigner rotation matrices are given in Table III. The conditional probability $P(\Omega_0 0 \,|\, \Omega t)$ that the orientation of the probe is Ω at time t given that it was Ω_0 at time 0, has the following properties

$$\lim_{t \to 0} P(\Omega_0 0 \,|\, \Omega t) = \delta(\Psi - \Psi_0)\delta(\Phi - \Phi_0)\delta(\theta - \theta_0)/\sin\theta \quad \text{(A3)}$$

$$\lim_{t \to \infty} P(\Omega_0 0 \,|\, \Omega t) = 4\pi^2 f(\theta) \quad \text{(A4)}$$

TABLE III
THE WIGNER ROTATION MATRIX ELEMENTS OF SECOND RANK $D^2_{mn}(\Omega) = e^{-im\Phi} d^{(2)}_{mn}(\theta) e^{-in\Psi}$, WHERE $d^{(2)}_{mn}(\theta)$ IS GIVEN IN THE TABLE

n \ m	−2	−1	0	1	2
−2	$\frac{1}{4}(1+\cos\theta)^2$	$-\frac{1}{2}(1+\cos\theta)\sin\theta$	$\sqrt{\frac{3}{8}}\sin^2\theta$	$-\frac{1}{2}(1-\cos\theta)\sin\theta$	$\frac{1}{4}(1-\cos\theta)^2$
−1	$\frac{1}{2}(1+\cos\theta)\sin\theta$	$\frac{1}{2}(-1+\cos\theta+2\cos^2\theta)$	$-\sqrt{\frac{3}{2}}\sin\theta\cos\theta$	$-\frac{1}{2}(1+\cos\theta-2\cos^2\theta)$	$-\frac{1}{2}(1-\cos\theta)\sin\theta$
0	$\sqrt{\frac{3}{8}}\sin^2\theta$	$\sqrt{\frac{3}{2}}\sin\theta\cos\theta$	$\frac{3}{2}\cos^2\theta - \frac{1}{2}$	$-\sqrt{\frac{3}{2}}\sin\theta\cos\theta$	$\sqrt{\frac{3}{8}}\sin^2\theta$
1	$\frac{1}{2}(1-\cos\theta)\sin\theta$	$\frac{1}{2}(1+\cos\theta-2\cos^2\theta)$	$\sqrt{\frac{3}{2}}\sin\theta\cos\theta$	$\frac{1}{2}(-1+\cos\theta+2\cos^2\theta)$	$-\frac{1}{2}(1+\cos\theta)\sin\theta$
2	$\frac{1}{4}(1-\cos\theta)^2$	$\frac{1}{2}(1-\cos\theta)\sin\theta$	$\sqrt{\frac{3}{8}}\sin^2\theta$	$\frac{1}{2}(1+\cos\theta)\sin\theta$	$\frac{1}{4}(1+\cos\theta)^2$

where $f(\theta)$ is the equilibrium singlet distribution function

$$f(\theta) = N \exp[-V(\theta)/kT] \tag{A5}$$

depending on the potential $V(\theta)$, the Boltzmann constant k, and the absolute temperature T. N is a normalization constant

$$N^{-1} = \int_0^\pi d\theta \sin\theta \exp(-V(\theta)/kT). \tag{A6}$$

The conditional probability is a solution of the Smoluchowski equation,

$$\dot{P}(\Omega_0 0 \,|\, \Omega t) = \Gamma P(\Omega_0 0 \,|\, \Omega t) \tag{A7}$$

with $\Gamma = L + K$ (A8a)

$$L = \frac{D_\perp}{\sin\theta}\frac{\partial}{\partial\theta}\sin\theta\left(\frac{\partial}{\partial\theta} + \frac{1}{kT}\frac{\partial V}{\partial\theta}\right) \tag{A8b}$$

$$K = \frac{D_\perp}{\sin^2\theta}\frac{\partial^2}{\partial\Phi^2} - D_\perp\frac{2\cos\theta}{\sin^2\theta}\frac{\partial^2}{\partial\Phi\partial\Psi} + D_\perp\left(\cot^2\theta + \frac{D_\parallel}{D_\perp}\right)\frac{\partial^2}{\partial\Psi^2}. \tag{A8c}$$

Taking the time derivative of $G_{mn}(t)$ in Eq. A1 at $t = 0$, and making use of Eqs. A7 and A3, we obtain

$$\begin{aligned}\dot{G}_{mn}(0) &= \frac{1}{4\pi^2}\int d\Omega_0 \int d\Omega\, D^2_{mn}(\Omega_0)^*\,\Gamma \\ &\quad \delta(\Psi - \Psi_0)\,\delta(\Phi - \Phi_0)\,\delta(\theta - \theta_0) \\ &\quad \times (\sin\theta)^{-1} f(\theta_0)\, D^2_{mn}(\Omega) \\ &= \frac{1}{4\pi^2}\int d\Omega\, D^2_{mn}(\Omega)^*\,\Gamma f(\theta)\, D^2_{mn}(\Omega)\end{aligned} \tag{A9}$$

which can be decomposed into

$$\dot{G}_{mnA} = \frac{1}{4\pi^2}\int d\Omega D^2_{mn}(\Omega)^*\, L f(\theta)\, D^2_{mn}(\Omega) \tag{A10a}$$

and

$$\dot{G}_{mnB} = \frac{1}{4\pi^2}\int d\Omega D^2_{mn}(\Omega)^*\, K f(\theta)\, D^2_{mn}(\Omega). \tag{A10b}$$

Employing the relation (9)

$$L D^2_{mn}(\Omega) f(\theta) = \frac{D_\perp}{\sin\theta}\frac{\partial}{\partial\theta}\sin\theta f(\theta)\frac{\partial}{\partial\theta} D^2_{mn}(\Omega) \tag{A11}$$

and integrating by parts, we find

$$\dot{G}_{mnA} = -D_\perp\left\langle \frac{\partial}{\partial\theta} D^2_{mn}(\Omega)^* \frac{\partial}{\partial\theta} D^2_{mn}(\Omega)\right\rangle \tag{A12}$$

using the single brackets as defined in Eq. 3. Evaluation of Eq. A10b gives

$$\dot{G}_{mnB} = -D_\perp\left\langle\left(\frac{m - n\cos\theta}{\sin\theta}\right)^2 D^2_{mn}(\Omega)^*\, D^2_{mn}(\Omega)\right\rangle - n^2 D_\parallel \langle D^2_{mn}(\Omega)^*\, D^2_{mn}(\Omega)\rangle. \tag{A13}$$

Because of the symmetry relation (10)

$$G_{mn}(t) = G_{-mn}(t) = G_{m-n}(t) = G_{-m-n}(t),$$

it suffices to evaluate $\dot{G}_{mn}(0)$ and $G_{mn}(0)$ for $m, n = 0, 1, 2$. These are given in Table I. The interpolation formulas used in Eq. 13 read

$$G_{mn}(t) = \langle P_2\rangle^2 \delta_{m,0}\,\delta_{n,0} + \beta_{mn}\exp(-\alpha_{mn}t). \tag{A14}$$

APPENDIX B

Here we show that the expression in Eq. A14 corresponds to an approximate solution of the Smoluchowski equation. The time derivatives of G_{mn} of higher order can be evaluated at $t = 0$ by extending the calculation performed in Eq. A9, allowing to write $G_{mn}(t)$ as a Taylor-series around $t = 0$

$$G_{mn}(t) = \sum_{l=0}^{\infty}\frac{t^l}{l!}\frac{1}{4\pi^2}\int d\Omega\, D^2_{mn}(\Omega)^*\,\Gamma^l f(\theta)\, D^2_{mn}(\Omega) \tag{B1}$$

from which the time derivative follows

$$\dot{G}_{mn}(t) = \sum_{l=0}^{\infty} l\frac{t^{l-1}}{l!}\frac{1}{4\pi^2}\int d\Omega\, D^2_{mn}(\Omega)^*\,\Gamma^l f(\theta)\, D^2_{mn}(\Omega). \tag{B2}$$

This can also easily be derived from the formal solution of Eq. A7, i.e., (20)

$$P(\Omega_0 0 \,|\, \Omega t) = \frac{\delta(\Omega - \Omega_0)}{\sin\theta}\exp(\Gamma t) \tag{B3}$$

By putting Eq. B3 in Eq. A1 and expanding the exponential one obtains Eq. B1. If G_{mn} decreases monotonously with time, t could be solved, in principal, as a function of G_{mn} and substituted into Eq. B2, yielding

$$\dot{G}_{mn} = H_{mn}[G_{mn} - G_{mn}(\infty)], \tag{B4}$$

where H_{mn} is the resulting functional, which is as yet unknown. Note that $H_{mn}(0) = 0$, because this corresponds to equilibrium. If $G_{mn}(t) - G_{mn}(\infty)$ is small, i.e., close to equilibrium, and/or H_{mn} is nearly linear, the following expansion is valid

$$\dot{G}_{mn}(t) = -\alpha_{mn}[G_{mn}(t) - G_{mn}(\infty)], \tag{B5}$$

where the coefficient α_{mn} is time independent, because it refers to equilibrium. Therefore, we have

$$\alpha_{mn} = -\dot{G}_{mn}(0)/[G_{mn}(0) - G_{mn}(\infty)]. \tag{B6}$$

The solution of Eq. B5 is

$$G_{mn}(t) = [G_{mn}(0) - G_{mn}(\infty)]\exp(-\alpha_{mn}t) + G_{mn}(\infty), \tag{B7}$$

which has the same form as in the extended strong collision model (10, 16). However, here the correlation times are not independent parameters, but are functions of $D_\perp$, $D_\parallel$, $\langle P_2\rangle$, and $\langle P_4\rangle$. The expressions for $G_{00}(t)$ and $G_{20}(t)$ have also been derived by Dozov and Penchev in a different way (21). In the case of free diffusion, $\langle P_{21}\rangle = 0$ for all $l \geq 1$, the approximation in Eq. B5 is exact.

APPENDIX C

The relevant formulas for the application of our second approximation (Eq. 14, the case that wobbling is dominant) to the phase and demodulation technique are the following

$$\text{excitation} \sim A + B\sin\omega t, \tag{C1}$$

where ω is the modulation frequency times 2π. The intensities for parallel ($\parallel$) and perpendicular ($\perp$) polarizers are proportional to

$$I_\parallel \sim A + BM_\parallel \sin(\omega t - \delta_\parallel) \tag{C2a}$$

$$I_\perp \sim A + BM_\perp \sin(\omega t - \delta_\perp), \tag{C2b}$$

where δ is the phase shift and M the modulation. The differential tangent and the modulation ratio are given by

$$\tan \Delta = \tan(\delta_\perp - \delta_\parallel) = \frac{3(\omega\tau C - S)}{(1 + 2r_\infty)(1 - r_\infty) + (1 - 4r_\infty)(C + \omega\tau S) - 2(1 + \omega^2\tau^2)(C^2 + S^2)} \quad \text{(C3)}$$

$$M_\parallel/M_\perp = \frac{1 - r_\infty - C_0}{1 + 2r_\infty + 2C_0} \times \sqrt{\frac{[1 + 2r_\infty + 2C(1 + \omega^2\tau^2)]^2 + [\omega\tau(1 + 2r_\infty) + 2S(1 + \omega^2\tau^2)]^2}{[1 - r_\infty - C(1 + \omega^2\tau^2)]^2 + [\omega\tau(1 - r_\infty) - S(1 + \omega^2\tau^2)]^2}} \quad \text{(C4)}$$

$$S = \frac{\omega\tau r_0\beta_{00}}{(1 + \alpha_{00}\tau)^2 + \omega^2\tau^2} + 2\omega\tau r_0 \sum_{i=1}^{2} \frac{\beta_{i0}}{(1 + \alpha_{i0}\tau)^2 + \omega^2\tau^2} \quad \text{(C5)}$$

$$C = \frac{r_0\beta_{00}(1 + \alpha_{00}\tau)}{(1 + \alpha_{00}\tau)^2 + \omega^2\tau^2} + 2r_0 \sum_{i=1}^{2} \frac{\beta_{i0}(1 + \alpha_{i0}\tau)}{(1 + \alpha_{i0}\tau)^2 + \omega^2\tau^2} \quad \text{(C6)}$$

$$C_0 = \frac{r_0\beta_{00}}{1 + \alpha_{00}\tau} + 2r_0 \sum_{i=1}^{2} \frac{\beta_{i0}}{1 + \alpha_{i0}\tau}. \quad \text{(C7)}$$

where τ is the fluorescence lifetime, $r_0 = r(0)$, $r_\infty = r(\infty)$ and the coefficients α_{i0} and β_{i0} ($i = 0, 1, 2$) are given in Table I.

Thanks are due to Dr. David Jameson (University of Texas, Dallas, TX) and Dr. Enrico Gratton (University of Illinois, Urbana, IL) for pointing out to us that the phase and demodulation technique could be appropriate to test our second approximation, if measurements would be performed at more than a few frequencies. Wieb van der Meer is supported by the Koningin Wilhelmina Fonds, Netherlands Cancer Foundation.

Received for publication 2 November 1983 and in final form 23 April 1984.

Note Added in Proof: After having submitted this paper, we received a preprint from Attila Szabo entitled "Theory of fluorescence depolarization in macromolecules and membranes" (1984, *J. Chem. Phys.* 81:150–167), in which similar results have been derived concerning the $\langle P_2 \rangle$ and $\langle P_4 \rangle$ dependence of the fluorescence anisotropy.

REFERENCES

1. Dale, R. E., L. A. Chen, and L. Brand. 1977. Rotational relaxation of the "microviscosity" probe diphenylhexatriene in paraffin oil and egg lecithin vesicles. *J. Biol. Chem.* 252:7500–7510.
2. Chen, L. A., R. E. Dale, S. Roth, and L. Brand. 1977. Nanosecond time-dependent fluorescence depolarization of diphenylhexatriene in dimyristoyllecithin vesicles and the determination of "microviscosity." *J. Biol. Chem.* 252:2163–2169.
3. Kawato, S., K. Kinosita, Jr., and A. Ikegami. 1977. Dynamic structure of lipid bilayers studied by nanosecond fluorescence techniques. *Biochemistry.* 16:2319–2324.
4. Lakowicz, J. R., F. G. Prendergast, and D. Hogen. 1979. Differential polarized phase fluorometric investigations of diphenylhexatriene in lipid bilayers. Quantitation of hindered polarizing rotations. *Biochemistry.* 18:508–519.
5. Kinosita, K., Jr., S. Kawato, and A. Ikegami. 1977. A theory of fluorescence depolarization decay in membranes. *Biophys. J.* 20:289–305.
6. Heyn, M. P. 1979. Determination of lipid order parameters and rotational correlation times from fluorescence depolarization experiments. *FEBS (Fed. Eur. Biochem. Soc.) Lett.* 108:359–364.
7. Jähnig, F. 1979. Structural order of lipids and proteins in membranes: Evaluation of fluorescence anisotropy data. *Proc. Natl. Acad. Sci. USA.* 76:6361–6365.
8. Lipari, G., and A. Szabo. 1980. Effect of librational motion on fluorescence depolarization and nuclear magnetic resonance relaxation in macromolecules and membranes. *Biophys. J.* 30:489–506.
9. Lipari, G., and A. Szabo. 1981. Padé approximants to correlation functions for restricted rotational diffusion. *J. Chem. Phys.* 75:2971–2976.
10. Zannoni, C. 1981. A theory of fluorescence depolarization in membranes. *Mol. Phys.* 42:1303–1320.
11. Zannoni, C., A. Arcioni, and P. Cavatorta. 1983. Fluorescence depolarization in liquid crystals and membrane bilayers. *Chem. Phys. Lipids.* 32:179–250.
12. Engel, L. W., and F. G. Prendergast. 1981. Values for and significance of order parameters and cone angles of fluorophore rotation in lipid bilayers. *Biochemistry.* 20:7338–7345.
13. Berne, B. J., P. Pechukas, and G. D. Harp. 1968. Molecular reorientation in liquids and gases. *J. Chem. Phys.* 49:3125–3129.
14. Ameloot, M., H. Hendrickx, W. Herreman, H. Pottel, F. Van Cauwelaert, and W. van der Meer. 1984. Effect of orientational order on the decay of the fluorescence anisotropy in membrane suspensions. Experimental verification on unilamellar vesicles and lipid/α-lactalbumin complexes. *Biophys. J.* 46:525–539.
15. Nordio, P. L., and U. Segre. 1979. Rotational dynamics. *In* The Molecular Physics of Liquid Crystals. G. R. Luckhurst and G. W. Gray, editors. Academic Press, Inc., New York. 411–426.
16. Luckhurst, G. R., M. Setaka, and C. Zannoni. 1974. An electron resonance investigation of molecular motion in the smectic A mesophase of a liquid crystal. *Mol. Phys.* 28:49–68.
17. Nordio, P. L., G. Rigatti, and U. Segre. 1972. Spin relaxation in nematic solvents. *J. Chem. Phys.* 56:2117–2127.
18. Kinosita, K., Jr., A. Ikegami, and S. Kawato. 1982. On the wobbling-in-cone analysis of fluorescence anisotropy decay. *Biophys. J.* 37:461–464.
19. Weber, G. 1978. Limited rotational motion recognition by differential phase fluorometry. *Acta Phys. Pol. Sect. A.* 54:859–865.
20. Szabo, A. 1980. Theory of polarized fluorescent emission in uniaxial liquid crystals. *J. Chem. Phys.* 72:4620–4626.
21. Dozov, I. N., and I. I. Penchev. 1980. Effect of the rotational depolarization in fluorescence measurements of the nematic order parameter. *J. Lumin.* 22:69–78.
22. Kooyman, R. P. H., Y. K. Levine, and W. van der Meer. 1981. Measurement of second and fourth rank order parameters by fluoresence polarization experiments in a lipid membrane system. *Chem. Phys.* 60:317–326.